

# Novel view of the origin of thermal and intrinsic breakdowns

AKIRA DOI

*Department of Materials, Nagoya Institute of Technology, Nagoya 466, Japan*

A novel view is presented on the origin of thermal and intrinsic breakdowns from the analysis of published data for pyrex glass and several polymers. For the former, the origin is not due to failure of thermal balance between joule heating and its dissipation, but to charge injection from the anode, by which the current surge to the cathode is afforded and, when the cathode cannot accommodate the neutralized charge carriers, those neutralized species would pile up and advance the cathode-front back to the anode and, finally, a filamentary conductive path is constructed between the electrodes. It is suggested that the occurrence of intrinsic breakdown is determined by the number of electrons which are injected from the cathode by tunnelling because an individual electron gives rise to a certain amount of damage on its passage through the insulator by momentum transfer. From the analysis of time delay before the onset of breakdown, we can estimate the electron affinity of an insulator.

## 1. Introduction

It is generally believed that dielectric breakdown of insulating materials can take place by either a thermal or an intrinsic mechanism. The latter breakdown can frequently be distinguished from the former by the fact that the dielectric strength,  $E_b$ , is insensitive or even increases with an increase in temperature, as shown schematically in Fig. 1.

A qualitative picture of thermal breakdown is: when a biasing field reaches a certain critical point, a thermal balance between joule heating and its dissipation through a dielectric is broken and the local temperature along a conduction path is increased, which in turn increases local electrical conductivity and local joule heating, so that eventually breakdown takes place as the material melts, cracks, burns, or vaporizes. However, it is also well known that when a high electric field is applied, e.g. to a glass, ionic species from the electrode material can be injected into and propagate through the glass as the extrinsic charge carriers for conduction [1-3]. Is there any relationship between those injected charge carriers and dielectric breakdown? In this paper we present a novel view of first the so-called thermal breakdown by re-analysing Vermeer's systematic work on pyrex glass [4], and second of the intrinsic breakdown by re-analysing data of several organic polymers.

## 2. Thermal breakdown

General results found from the thermally stimulated polarization/depolarization current measurements of gold- or silver-electroded  $\text{Li}_2\text{O} \cdot 2\text{SiO}_2$  glass, in the temperature range up to 500 K with an applied field of  $200 \text{ V cm}^{-1}$ , are [3]: (1) gold acts as a totally blocking anode, so an alkali-depleted region (ADR) containing negative space charge is developed near the anode by lithium depletion; (2) the ADR thickness, found from

secondary-ion mass spectroscopic measurements, is of comparable magnitude with that estimated based on the assumptions that the total electric current is carried solely by lithium ions, and those lithium ions which are neutralized at the cathode are equivalent in number to those which are depleted from ADR; (3) when silver instead of gold is used as the anode, silver ions can be injected into glass and reduce the potential drop at ADR drastically. Moreover, even a gold anode can inject gold ions into  $\text{Li}_2\text{O} \cdot 2\text{SiO}_2$  [1] and silica [2] glasses when the temperature is above  $500^\circ \text{C}$ , or into  $\text{Li}_2\text{O} \cdot 2\text{SiO}_2$  glass at room temperature when the applied field is above  $50 \text{ kV cm}^{-1}$  [3].

As long as the anode is totally blocking, ADR develops near the anode and a potential drop across it retards electrical conduction of the glass bulk. If, on the other hand, the anode could inject ions into glass by an extremely high field, the potential drop at ADR would be decreased and conduction would continue. With such a quasi-ohmic contact at the glass-anode interface, the ionic charge carriers move to the cathode where they are neutralized. The neutral atoms may diffuse into the electrode [5] or, when the amount of solute exceeds the solubility limit of the electrode material and/or when the rate of impingement of the charge carriers into the cathode is too much for accommodation, those neutralized species will be piled up on the cathode surface and develop the cathode-front. By the growth of the cathode-front back to the anode, the effective field within the glass bulk increases. Correspondingly, electrical conduction increases, which accelerates the growth of the cathode-front and, finally, breakdown takes place by the formation of a conductive filament between the electrodes. This filament may not necessarily be a metallic whisker but can be a compound generated by chemical reaction at the cathode-front. The

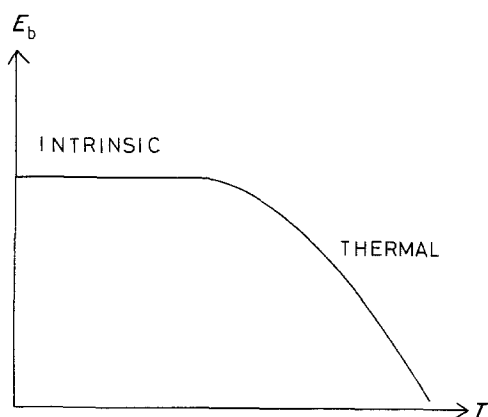


Figure 1 A schematic drawing of the variation of dielectric strength,  $E_b$ , with temperature, showing intrinsic and thermal breakdown regions.

occurrence of breakdown by the formation of filamentary conductive paths is already demonstrated by the switching of chalcogenide glasses.

Vermeer's experimental procedure was to measure a breakdown voltage during the course of which an applied voltage was increased from zero to a predetermined value about 1.5 times the expected breakdown voltage, with various voltage rise times. It was shown that  $E_b$  decreases with increasing  $t^*$ , the voltage rise time. Assume then that  $t^*$  is proportional to a time required for the growth of the cathode-front back to the anode, although the growth may be taking place in a time much shorter than  $t^*$ , with zero growth over a large part of the prebreakdown period. The drift velocity of the charge carriers is given by [6]

$$\begin{aligned} v &\cong \lambda v \exp \{-(H - eE\lambda/\alpha)/kT\} \\ &= \text{const} \exp (eE\lambda/\alpha kT) \end{aligned} \quad (1)$$

for a given temperature and when the applied field,  $E$ , is extremely high ( $eE\lambda \gg \alpha kT$ ). Because the time for the growth of the cathode-front to the anode must be inversely proportional to the drift velocity,  $t^*$  can be described as

$$t^* \cong t_0 \exp (-eE_b\lambda/\alpha kT) \quad (2)$$

where  $\lambda$  is the jump distance,  $\alpha$  the number of possible jump directions,  $v$  the oscillation frequency of the charge carriers,  $H$  the activation energy for conduction, and  $E_b$  the dielectric strength. Fig. 2 illustrates the validity of Equation 2 for pyrex glass, showing that  $\log t^*$  is proportional to  $E_b$  with a slope  $e\lambda/\alpha kT$  decreasing with an increase in temperature. Departures from linearity at high temperature and low field may be due to a failure of the aforementioned high-field approximation. When  $\log t^*$  was plotted as a function of reciprocal temperature at an arbitrarily chosen  $E_b$  in the linear regions, say at  $8.5 \times 10^6 \text{ V cm}^{-1}$ , we found a linear relationship (Fig. 3). The jump distance is estimated from the slope  $eE_b\lambda/\alpha k$  to be 1.7 nm, when 2 is taken as equal to  $\alpha$  which may be reasonable for an extremely high field. On the other hand, the average jump distance of sodium ions in the pyrex glass is estimated from

$$\lambda_{\text{av}} = \left( \frac{6}{\pi N} \right)^{1/3} \quad (3)$$

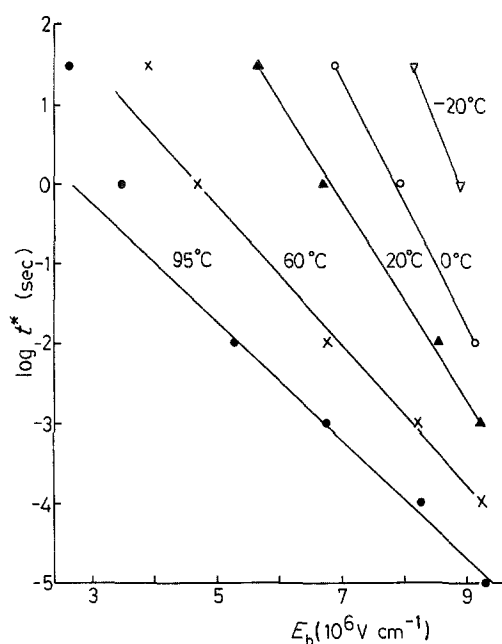


Figure 2 Logarithmic voltage rise time,  $t^*$ , as a function of dielectric strength for pyrex glass at several temperatures [4]. Specimen thickness  $25 \mu\text{m}$ .

to be 1.3 nm, by assuming homogeneous distribution of sodium ions with nominal density  $N$  of  $8.9 \times 10^{20} \text{ cm}^{-3}$ . In view of several assumptions inherent in our derivation, the agreement is excellent. That  $E_b$  was insensitive to thickness over the range, say, 20 to  $70 \mu\text{m}$  [4] is consistent with our model that "thermal" breakdown is caused by ionic conduction governed by the applied field, not by the applied voltage.

A difference in the  $t^*$ -dependences of the dielectric strength for different electrode materials [4, 7] may be the reflection of different injection feasibilities. For example, that the dielectric strength for any given  $t^*$  within the range of "thermal" breakdown was smaller for silver-electroded samples than for the samples with  $\text{CuSO}_4$ -aqueous electrodes (Fig. 4 [4]) is in agreement with our general belief that silver, compared to copper, can more easily be injected into glass.

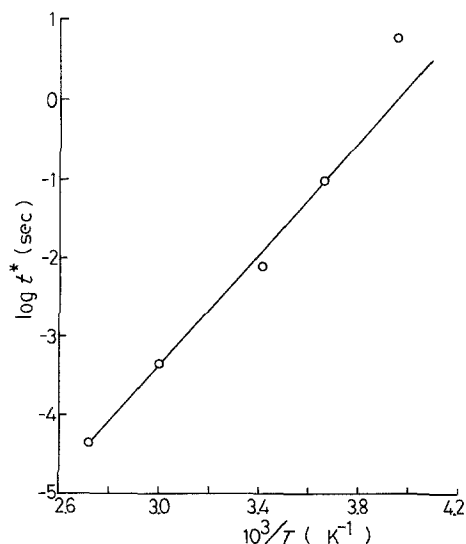


Figure 3 Logarithmic voltage rise time,  $t^*$ , as a function of reciprocal temperature at an arbitrarily chosen dielectric strength of  $8.5 \times 10^6 \text{ V cm}^{-1}$  at which linearity is found as in Fig. 2.

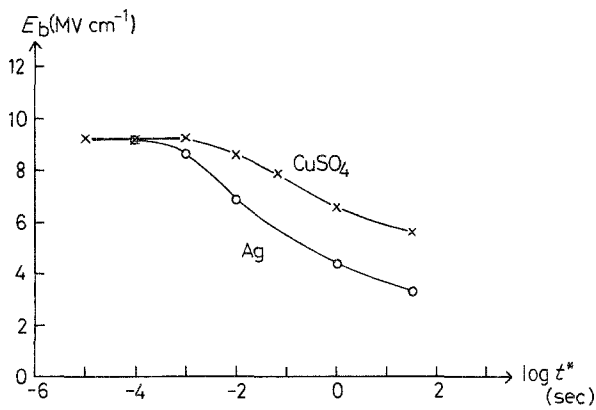


Figure 4 Temperature dependences of dielectric strength for pyrex glass samples with silver and  $\text{CuSO}_4$ -aqueous electrodes [4].

### 3. Intrinsic breakdown

Curves in Fig. 2 converge to a point with  $t^* \sim 10^{-7}$  sec and  $E_b \sim 12 \times 10^6 \text{ V cm}^{-1}$ . However, Vermeer [4] found that the dielectric strength converged with decreasing  $t^*$  to a constant value of  $9.2 \times 10^6 \text{ V cm}^{-1}$ , irrespective of temperatures between  $-55$  and  $+95^\circ \text{C}$ . This implies that another breakdown mechanism, possibly the electron avalanche mechanism of intrinsic or electric breakdown, emerges before the dielectric strength due to "thermal" breakdown reaches its uppermost value. Because the field emission of electrons occurs at a field of  $\sim 10^7 \text{ V cm}^{-1}$ , it is possible that the temperature-independent, so-called intrinsic, breakdown may be related to field emission. Because of the lack of systematic studies on intrinsic breakdown of glass, intrinsic breakdown of organic polymers will be discussed.

The temperature-dependence of  $E_b$  for organic polymers also follows the curves as shown in Fig. 1. For many polymers a critical temperature, above which the breakdown is due predominantly to a thermal origin, is near the glass transition temperature,  $T_g$  [8]. Within temperature ranges where intrinsic breakdown prevails, the time lags before the onset of breakdown were measured by e.g. Inuishi and co-workers [9, 10] for high-density polyethylene (HDPE) and polyethylene terephthalate (PET), when a step voltage with a rise time as short as 1 nsec was applied. Empirically the number of the samples,  $n_i$ , which do not suffer breakdown within a time lag  $\delta$ , is given by

$$n_i/n_0 = \exp [-(\delta - t_f)/t_s] \quad (4)$$

where  $n_0$  is the overall number of the samples and  $t_f$  and  $t_s$  are the adjustable parameters which depend on the applied field. Therefore, for a given value of  $n_i/n_0$ ,  $\delta$  varies with the applied field.

The intrinsic breakdown is believed, generally, to arise from the electron avalanche mechanism which involves creation of an electron-hole pair by the scattering of individual electrons having kinetic energies exceeding the band gap as a result of runaway processes in high fields after tunnelling from the cathode. The number density of tunnelling electrons per second is given by [9]

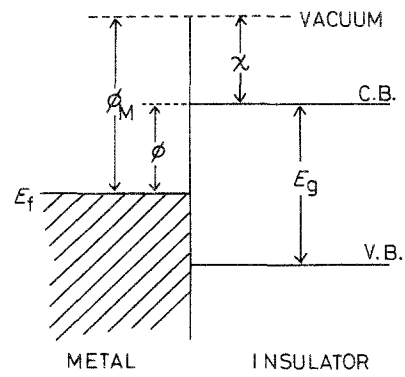


Figure 5 Energy diagram at the metal-insulator interface, where  $E_f$  is the Fermi level,  $\phi_m$  the metal work function,  $\phi$  the energy barrier for the Fermi electrons of the metal to the conduction band edge (C.B.) of an insulator, V.B. the valence band edge,  $E_g$  the band gap, and  $\chi$  the electron affinity of an insulator.

$$N = \frac{2.2e^2 E_b^2}{8\pi h \phi} \exp \left[ -\frac{8\pi(2m\phi^3)^{1/2}}{2.96heE_b} \right] \quad (5)$$

where

$$\phi = \phi_m - \chi \quad (6)$$

is the difference in the metal work function,  $\phi_m$ , and the electron affinity of the insulator,  $\chi$  (Fig. 5).

A Monte Carlo simulation of hot electron trajectories in the conduction band of  $\text{SiO}_2$  [11] reveals that for fields above  $2 \times 10^6 \text{ V cm}^{-1}$ , large-angle scattering by acoustic phonons stabilizes electron energies and produces diffusive trajectories. If damage caused by such a momentum transfer is a prerequisite for intrinsic breakdown, the amount of damage would be proportional to  $N\delta$ , the total number of electrons injected into an insulator. That is,  $N\delta$  can be a criterion for the onset of intrinsic breakdown with a probability of  $1 - n_i/n_0$ . Then, from Equation 5,

$$\ln \delta = \text{const} + c/E_b \quad (7)$$

where

$$c = 8\pi(2m\phi^3)^{1/2}/2.96he \quad (8)$$

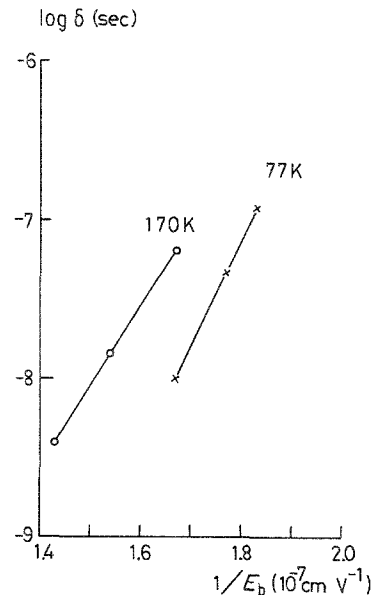


Figure 6 Logarithmic time delay,  $\delta$ , as a function of reciprocal dielectric strength for gold-electroded HDPE at two different temperatures [10].

TABLE I Electron affinities,  $\chi$ , for HDPE and PET, as estimated from time-delay analyses of intrinsic breakdown at several temperatures of the samples with gold and aluminium electrodes

			Temperature (K)			Average $\chi$ (eV)	
			77	170	293		
HDPE	Au	$\phi$	1.70	1.42			
		$\chi$	3.4	3.7			
	Al	$\phi$	$0.92 \pm 0.04$	$1.16 \pm 0.04$		$3.4 \pm 0.3$	
		$\chi$	3.4	3.1			
PET	Au	$\phi$			$2.1 \pm 0.3$		
		$\chi$			$3.0 \pm 0.3$		
	Al	$\phi$			$1.7 \pm 0.4$	$2.8 \pm 0.6$	
		$\chi$			$2.6 \pm 0.4$		

At an arbitrarily chosen value of  $n_i/n_0$ , say 0.60, gold-electroded HDPE fits well to Equation 7, as shown in Fig. 6, but not so well for others. Because the work functions for gold and aluminium are 5.1 and 4.28 eV, respectively [12], we can determine the electron affinities for HDPE and PET from the slopes of the  $\ln \delta$  against  $1/E_b$  plots (Table I). The value of  $\chi$  for PET ( $2.8 \pm 0.6$  eV) is not very different from the estimated values, 2.0 ~ 2.3 eV [13]. Downward depression of the curves with decreasing temperature, as shown in Fig. 6, would mean a reduction of the critical number of electrons for the onset of breakdown, or the reduction of  $E_b$  as we sometimes observed for the intrinsic breakdown.

It is interesting to note that  $E_b$  for hexatriacontane ( $C_{36}H_{74}$ ) single crystal is temperature-insensitive up to its melting point [14], that is, this single crystal does not show thermal breakdown. It is suggested that thermal breakdown or the relevant ionic conduction would take place mainly in the amorphous phase and, at least for polymers, at temperatures above  $T_g$ . Because  $T_g$  is a temperature at which frozen-in motion of the carbon chains is loosened, some of the constituents would be freed and become the charge carriers for conduction.

In summary, it is suggested that a criterion for the onset of intrinsic breakdown is the number of electrons

which are injected from the cathode into the conduction band of an insulator by tunnelling and cause damage by momentum transfer. We can determine the electron affinity of an insulator by the measurements of time delay.

## References

1. C. KIM and M. TOMOZAWA, *J. Amer. Ceram. Soc.* **59** (1976) 321.
2. T. W. HICKMOTT, *J. Appl. Phys.* **51** (1980) 4269.
3. A. DOI, T. MIWA and A. MIZUIKE, *J. Mater. Sci.* **20** (1985) 1787.
4. J. VERMEER, *Physica* **20** (1954) 313.
5. K. TAKIZAWA, *J. Amer. Ceram. Soc.* **61** (1978) 475.
6. A. E. OWEN, in "Progress in Ceramic Science", Vol. 3, edited by J. E. Burke (Pergamon, New York, 1963) p. 84.
7. J. VERMEER, *Physica* **22** (1956) 1247.
8. M. IEDA, *IEEE Trans. Elect. Insul.* **EI-15** (1980) 206.
9. K. ARII, I. KITANI and Y. INUISHI, *Trans. IEE Jpn* **93-A** (1973) 313.
10. K. ARII and I. KITANI, *ibid.* **94-A** (1974) 251.
11. M. V. FISCHETTI, D. J. DIMARIA, S. D. BRORSON, T. N. THEIS and J. R. KIRTLEY, *Phys. Rev.* **B31** (1985) 8124.
12. H. B. MICHAELSON, *J. Appl. Phys.* **48** (1977) 4729.
13. A. C. LILLY Jr, *ibid.* **41** (1970) 2001.
14. K. YOSHINO, S. HARADA, J. KYOKANE and Y. INUISHI, *J. Phys.* **D12** (1979) 1535.

Received 27 January

and accepted 15 April 1987